

1 **Supporting Information**

2 **Where the river turns old: Urbanized deltas imprint a fossil signature**

3 **on black carbon exported to the ocean**

4 Xin Yi^{1,2}, Xiaofei Geng^{1,3}, Guangcai Zhong^{1,*}, Bolong Zhang¹, Sanyuan Zhu¹,
5 Hongxing Jiang¹, Yangzhi Mo¹, Shizhen Zhao¹, Jun Li¹, Huizheng Che², Gan Zhang^{1,*}

6

7 ¹ State Key Laboratory of Advanced Environmental Technology (SKLAET) and
8 Guangdong-Hong Kong-Macao Joint Laboratory for Environmental Pollution and
9 Control, Guangzhou Institute of Geochemistry, Chinese Academy of Sciences,
10 Guangzhou, 510640, China

11 ² State Key Laboratory of Severe Weather Meteorological Science and Technology
12 (LaSW) & Key Laboratory of Atmospheric Chemistry of CMA, Chinese Academy of
13 Meteorological Sciences, Beijing, 100081, China

14 ³ School of Marine Sciences, Hainan University, Haikou, 570228, China

15

16 *Corresponding Author: Dr. Gan Zhang

17 Tel: +86-20-85290805; fax: +86-20-85290706; e-mail: zhanggan@gig.ac.cn

18 *Corresponding Author: Dr. Guangcai Zhong

19 Tel: +86-20-38350480; fax: +86-20- 38350480; e-mail: gczhong@gig.ac.cn

20

21 **Content: 22 pages, 6 texts, 7 tables, and 2 figures**

22 **List of Contents:**

23 **Supplementary Texts**

24 **Text S1.** SPE-DOC extraction and carbon content measurements

25 **Text S2.** Stable carbon ($\delta^{13}\text{C}$) and radiocarbon ($\delta^{14}\text{C}$) analysis of SPE-DOC and POC

26 **Text S3.** Parameter calculations for FT-ICR-MS

27 **Text S4.** Concentration measurements of DBC and PBC

28 **Text S5.** Preparative high-performance liquid chromatography (prep-HPLC)

29 **Text S6.** Stable carbon isotope analysis ($\delta^{13}\text{C}$) of DBC and PBC

30 **Supplementary Tables**

31 **Table S1.** Information on eight sampling sites during the first sampling campaign. The
32 commercial, industrial, and residential areas, as well as the road length, are data within
33 5 km of each sampling site.

34 **Table S2.** Binary gradient of HPLC method for BPCA quantification.

35 **Table S3.** Binary gradient of preparative high-performance liquid chromatography
36 (prep-HPLC).

37 **Table S4.** Concentrations of DOC and POC, and $\delta^{13}\text{C}$ - $\Delta^{14}\text{C}$ of SPE-DOC and POC
38 along the urbanization gradient of the Liuxi River.

39 **Table S5.** BPCAs Concentrations of DBC along the urbanization gradient of the Liuxi
40 River.

41 **Table S6.** BPCAs Concentrations of PBC along the urbanization gradient of the Liuxi
42 River.

43 **Table S7.** Dual-carbon isotopic compositions ($\Delta^{14}\text{C}$ - $\delta^{13}\text{C}$) of DBC and PBC at the
44 upper reach (forest site) and lower reach (urban site).

45 **Supplementary Figures**

46 **Figure S1.** Monthly precipitation during the second sampling campaign (May 2021 to
47 April 2022) of Guangzhou.

48 **Figure S2.** DOM molecular compositions along the urbanization gradient of the Liuxi
49 River.

50 **References**

51

52 **Supplementary Texts**

53 **Text S1. SPE-DOC extraction and carbon content measurements**

54 DOC was isolated from water samples using solid phase extraction (SPE).¹ Briefly,
55 prepacked SPE cartridges (Varian Bond Elut PPL cartridges, Agilent, the US) were
56 conditioned with methanol and HCl (pH = 2). Filtered and acidified water samples were
57 siphoned through the SPE cartridge with a cleaned PTFE (polytetrafluoroethylene) tube
58 at a slow loading rate (<20 mL min⁻¹). This flow rate was monitored and maintained
59 throughout the sample loading. After extraction, the cartridge sorbent was rinsed with
60 two bed-volume of HCl (pH = 2) to remove salts, then the PPL cartridge was freeze-
61 dried. Isolated DOC was eluted from the SPE cartridge with two bed-volume methanol.
62 The methanol eluent was then condensed to ~5 mL via a rotary evaporator.

63 To determine the carbon content of SPE-DOC, an aliquot of the methanol eluent
64 was transferred to a 20-mL glass bottle and dried under a stream of high-purity nitrogen
65 gas at 40 °C. The residue was redissolved in 10 mL ultrapure water (18.2 MΩ cm⁻¹,
66 Sartorius), and the carbon content was quantified following the same method as DOC.

67

68 **Text S2. Stable carbon ($\delta^{13}\text{C}$) and radiocarbon ($\delta^{14}\text{C}$) analysis of SPE-DOC and**
69 **POC**

70 The $\delta^{13}\text{C}$ of SPE-DOC and POC were determined by elemental analysis-isotope
71 ratio mass spectrometry (EA-IRMS). The methanol eluent containing 20–40 $\mu\text{g C}$ SPE-
72 DOC was weighed into tin boats and evaporated to dryness in an oven at 60 °C. Then
73 the tin boats were folded and combusted using a Thermo Scientific Flash Elemental
74 Analyser interfaced with a Thermo Scientific Delta V Plus IRMS. A two-point
75 calibration was performed to calculate the $\delta^{13}\text{C}$ values using two international reference
76 standards (USGS40, $\delta^{13}\text{C} = -26.39 \pm 0.04\text{\textperthousand}$; IAEA-CH-6, $\delta^{13}\text{C} = -10.45 \pm 0.04\text{\textperthousand}$)².
77 A working standard (Casein standard OAS, CatNo. B2155-Batch no. 2821, $\delta^{13}\text{C} = -$
78 $26.98 \pm 0.13\text{\textperthousand}$, Elemental Microanalysis Ltd) was used for routine quality assurance.
79 For POC analysis, the GF/F filters containing particulate material were treated with
80 concentrated HCl (36%) vapor in a desiccator for at least 24 h to completely remove
81 carbonates. After freeze-drying, organic matters were scraped off the filters, transferred
82 into tin boats, and analyzed by EA-IRMS.

83 In similar procedures to $\delta^{13}\text{C}$ analysis, the SPE-DOC and POC samples were
84 packed into the tin boats and combusted at 900 °C for 2.5 h to oxidize into CO_2 , which
85 was then reduced to graphite using hydrogen at 525 °C for 3 h over iron catalysts.³ The
86 graphite was pressed into aluminum targets for $\Delta^{14}\text{C}$ measurement with AMS at the
87 Guangzhou Institute of Geochemistry, Chinese Academy of Sciences.⁴

89 **Text S3. Parameter calculations for FT-ICR-MS**

90 The modified aromatic index (AI_{mod}) is calculated using the equation:^{5 6}

91
$$AI_{mod} = (1 + c - 0.5o - s - 0.5h) / (c - 0.5o - s - n)$$

92 In order to consider the intensity of each formula and its contribution to the overall
93 property, the intensity-weighted AI_{mod} (AI_{mod-w}) and elemental ratio (H/C_{-w} and O/C_{-w})
94 were calculated based on the following equations.^{7, 8}

95
$$AI_{mod-w} = \sum (In_i \times AI_{mod i}) / \sum In_i$$

96
$$H/C_{-w} = \sum (In_i \times H/C_i) / \sum In_i$$

97
$$O/C_{-w} = \sum (In_i \times O/C_i) / \sum In_i$$

98 Where AI_{mod i}, H/C_i, and O/C_i represent the AI_{mod}, H/C, and O/C of the individual
99 molecular formula (i), respectively, In_i is the intensity for individual molecular formula
100 (i), and i is the total number of identified molecular formulas in a given sample.

101

102 **Text S4. Concentration measurements of DBC and PBC**

103 Both DBC and PBC were determined using the BPCA method following our
104 previous studies.⁹⁻¹¹ Briefly, SPE-DOC extracts (~500 mL water sample equivalents)
105 were transferred into a 10 mL ampoule and dried at 40 °C under high-purity nitrogen
106 blowing. Concentrated nitric acid (2 mL, 65%, p.a., Sigma Aldrich) was added to each
107 ampule, then the ampules were flame-sealed and heated to 180 °C for 8 h. After
108 oxidation, the solutions were dried under high-purity nitrogen at 50 °C. The BPCA-
109 containing residue was re-dissolved in ultrapure water and filtered with a syringe filter
110 (13 mm × 0.22 µm, PTFE, ANPEL Laboratory Technologies) for further analysis.

111 For PBC analysis, the GF/F filters containing particulate material were treated
112 with concentrated HCl (36%) vapor in a desiccator for at least 24 h to completely
113 remove carbonates. After freeze-drying, organic matters were scraped off the filters and
114 transferred into a 10 mL ampoule. Concentrated nitric acid (2 mL) was added to each
115 ampule. The ampoules were flame-sealed and heated to 180 °C for 8 h. After oxidation,
116 the sample solutions were dried under a stream of high-purity nitrogen gas at 50 °C.
117 The dried samples were re-dissolved in ultrapure water and passed through a glass
118 column packed with cation exchange resin (Dowex 50 WX8 400, Sigma Aldrich) to
119 remove extensive metal ions.¹²⁻¹⁴ The eluate was freeze-dried and re-dissolved in
120 ultrapure water, followed by filtration with a syringe filter (13 mm × 0.22 µm, PTFE,
121 ANPEL Laboratory Technologies) for further analysis.

122 BPCAs were separated on an Agilent InfinityLab Poroshell 120 SB-C18 (4.6 ×
123 100 mm, 2.7 µm, the US) column and quantified by a high-performance liquid

124 chromatography system equipped with a photodiode array detector (HPLC-PAD,
125 Shimadzu, Japan). Mobile phase A was an aqueous solution prepared by mixing 20 mL
126 of phosphoric acid (85%; Sigma-Aldrich) in 980 mL ultrapure water. HPLC-grade
127 acetonitrile (Sigma-Aldrich) was used as mobile phase B. The mixing gradients of
128 mobile phases A and B are shown in [Table S2](#). The flow rate and column oven
129 temperature were 0.4 mL min/L and 30 °C, respectively. Peak identifications of BPCAs
130 in samples were based on the retention times and absorbance spectra (190–400 nm).

131 The intensities of BPCA peaks at a wavelength of 240 nm were used for quantification.

132 Seven BPCAs were quantified, including 1,2,3,4,5,6-benzenehexacarboxylic acid
133 (B6CA), 1,2,3,4,5-benzenepentacarboxylic acid (B5CA), 1,2,4,5-
134 benzenetetracarboxylic acid, 1,2,3,5-benzenetetracarboxylic acid, 1,2,3,4-
135 benzenetetracarboxylic acid (B4CAs), 1,2,3-benzenetricarboxylic acid, and 1,2,4-
136 benzenetricarboxylic acid (B3CAs). A conversion factor of 5.7 from BPCAs-C to PBC
137 was used to calculate PBC concentrations based on our previous study.^{9, 15, 16} DBC
138 concentrations were calculated using the established relationship between DBC and
139 BPCAs shown below.¹⁷

$$140 [PBC] = 5.7 \times ([B6CA] + [B5CA] + [B4CAs] + [B3CAs])$$

$$141 [DBC] = 33.4 \times ([B6CA] + [B5CA] + 0.5 \times [B4CAs] + 0.5 \times [B3CAs])$$

142 The units of PBC(DBC) and BPCA are μM-C and μM, respectively. It is worth
143 noting that there are no two commercially available standards for 1,2,3,5-B4CA and
144 1,2,3,4-B4CA, these two B4CAs were quantified using the calibration curve of their
145 isomer (i.e., 1,2,4,5-B4CA).

146

147 **Text S5. Preparative high-performance liquid chromatography (prep-HPLC)**

148 In a procedure similar to the concentration measurement, DBC and PBC samples
149 were oxidized with concentrated nitric acid. After drying the oxidized solutions, the
150 samples were re-dissolved in ultrapure water and passed through a cation exchange
151 column (Dowex 50 WX8 400). The eluate was freeze-dried and re-dissolved in 0.38%
152 TFA (mobile phase A of prep-HPLC), followed by filtration with a syringe filter (13
153 mm × 0.22 µm, PTFE). BPCAs were separated with an Agilent Poroshell 120 SB-C18
154 (4.6 × 150 mm, 2.7 µm, the US) column and collected by a preparative liquid
155 chromatography using an HPLC system equipped with a photodiode array detector
156 (prep-HPLC-PAD, LC-20AT/SPD-M20A, Shimadzu). Mobile phase A was prepared by
157 mixing 3.8 mL trifluoroacetic acid (TFA) in 1 L ultrapure water (pH~1.3), acetonitrile
158 was used as mobile phase B. The mixing gradients of mobile phases A and B are shown
159 in [Table S3](#). It took a total run time of 62.10 min. Flow rate and column oven
160 temperature were 0.4 mL min⁻¹ and 30 °C. Individual BPCA was collected in a separate
161 glass tube via a fraction collector (FRC-10A, Shimadzu). The collected fractions were
162 put into 25-mL glass flasks and concentrated to ~1 mL using a rotary evaporator. They
163 were then transferred to 1.5 mL glass vials and dried under high-purity nitrogen
164 (99.999%) gas at 70 °C for 1 h. B4CA isomers were pooled together for subsequent
165 isotopic analysis. B3CAs were not collected due to their low abundance.
166

167 **Text S6. Stable carbon isotope analysis ($\delta^{13}\text{C}$) of DBC and PBC**

168 The $\delta^{13}\text{C}$ measurements of BPCAs were performed on an UltiMate 3000 HPLC
169 system connected to a Delta V Plus IRMS via an Isolink interface (HPLC-IRMS,
170 Thermo Scientific). Before $\delta^{13}\text{C}$ analysis, the isolated BPCA was redissolved in 0.5 mL
171 of ultrapure water and sonicated for 5 min to ensure complete dissolution. The HPLC-
172 IRMS setup was as follows: Ultrapure water was used as the mobile phase at a flow
173 rate of 200 $\mu\text{L}/\text{min}$. Online oxidation quantitatively converted individual BPCA to CO_2
174 in the Isolink oxidation chamber (98 °C) by adding H_3PO_4 and oxidant ($\text{Na}_2\text{S}_2\text{O}_8$). The
175 flow rates of acid and oxidant were optimized to yield an O_2 signal ($\text{m/z} = 32$) of 8–12
176 V to ensure full oxidation capacity. The derived CO_2 was then extracted from the mobile
177 phase and dried prior to detection by IRMS.

178 The HPLC-IRMS system did not require an LC column because of the preliminary
179 isolation of individual BPCA, which took only 6.5 min for each measurement run. A
180 two-point calibration was performed to calculate the BPCA- $\delta^{13}\text{C}$ values with two
181 international reference standards (USGS40, $\delta^{13}\text{C} = -26.39 \pm 0.04\text{\textperthousand}$; IAEA-CH-6, $\delta^{13}\text{C}$
182 $= -10.45 \pm 0.04\text{\textperthousand}$). BPCA standards were analyzed daily before sample analysis to
183 assess the stability of HPLC-IRMS.

184

185 **Supplementary Tables**186 **Table S1. Concentrations of DOC and POC, and $\delta^{13}\text{C}$ - $\Delta^{14}\text{C}$ of SPE-DOC and POC along the urbanization gradient of the Liuxi River.**

Sample ID From upstream to downstream	Dissolved Phase						Particulate Phase					
	DOC ($\mu\text{M-C}$)		$\delta^{13}\text{C}_{\text{SPE-DOC}} (\text{\textperthousand})$		$\Delta^{14}\text{C}_{\text{SPE-DOC}} (\text{\textperthousand})$		POC ($\mu\text{M-C}$)		$\delta^{13}\text{C}_{\text{POC}} (\text{\textperthousand})$		$\Delta^{14}\text{C}_{\text{POC}} (\text{\textperthousand})$	
	Wet season	Dry season	Wet season	Dry season	Wet season	Dry season	Wet season	Dry season	Wet season	Dry season	Wet season	Dry season
1	50.60	44.17	-28.60	-29.05	-62.82	-90.98	77.33	16.62	-27.79	-28.59	-77.40	-236.25
2	52.77	45.56	-28.41	-28.87	-78.43	-114.76	40.44	12.34	-29.16	-27.04	-84.54	-218.85
3	64.97	51.38	-28.42	-28.77	-73.66	-94.72	441.39	36.80	-27.38	-27.07	-54.23	-144.09
4	76.42	56.67	-28.36	-28.27	-80.00	-124.34	166.63	62.17	-29.15	-27.06	-53.91	-198.39
5	88.06	65.56	-28.14	-28.07	-110.14	-122.83	137.56	175.85	-32.16	-26.89	-64.50	-164.83
6	111.11	68.61	-27.48	-28.06	-139.10	-159.49	192.88	28.54	-24.94	-27.84	-67.49	-200.85
7	123.06	88.33	-27.63	-27.85	-167.00	-186.42	272.58	35.55	-30.74	-28.12	-86.74	-246.64
8	154.17	122.50	-27.20	-27.38	-177.78	-205.77	255.69	138.65	-29.86	-27.55	-156.89	-274.13
Average	90.14 ± 36.66	67.85 ± 26.37	-28.03 ± 0.52	-28.29 ± 0.57	-111.12 ± 44.92	-137.41 ± 42.15	198.06 ± 126.59	63.32 ± 60.71	-28.90 ± 2.21	-27.52 ± 0.61	-80.71 ± 33.22	-210.51 ± 42.80

Table S2. BPCAs Concentrations of DBC along the urbanization gradient of the Liuxi River.

Sample ID From upper reaches to lower reaches	Wet season					Dry season				
	B3CAs ($\mu\text{g/L}$)	B4CAs ($\mu\text{g/L}$)	B5CAs ($\mu\text{g/L}$)	B6CAs ($\mu\text{g/L}$)	DBC ($\mu\text{mol/L}$)	B3CAs ($\mu\text{g/L}$)	B4CAs ($\mu\text{g/L}$)	B5CAs ($\mu\text{g/L}$)	B6CAs ($\mu\text{g/L}$)	DBC ($\mu\text{mol/L}$)
1	0.37	3.34	2.83	0.92	1.45	0.34	2.59	2.26	0.79	1.17
2	0.43	3.68	3.03	0.97	1.57	0.45	3.15	2.74	0.92	1.42
3	0.52	4.72	4.34	1.25	2.13	0.38	3.17	3.83	0.99	1.70
4	0.66	6.04	4.85	1.38	2.49	0.59	4.71	4.41	1.37	2.18
5	0.99	9.21	7.19	2.00	3.72	0.66	5.07	5.43	1.70	2.58
6	1.13	9.92	7.95	2.08	4.05	0.62	4.92	4.00	1.29	2.09
7	1.49	13.18	9.33	2.58	5.02	0.74	5.74	4.59	1.55	2.43
8	2.09	17.57	12.22	3.63	6.70	1.11	10.00	7.65	2.20	4.01
Average	0.96 ± 0.60	8.46 ± 5.03	6.47 ± 3.30	1.85 ± 0.93	3.39 ± 1.84	0.61 ± 0.25	4.92 ± 2.33	4.36 ± 1.67	1.35 ± 0.46	2.20 ± 0.88

Table S3. BPCAs Concentrations of PBC along the urbanization gradient of the Liuxi River.

Sample ID From upper reaches to lower reaches	Wet season					Dry season				
	B3CAs ($\mu\text{g/L}$)	B4CAs ($\mu\text{g/L}$)	B5CAs ($\mu\text{g/L}$)	B6CAs ($\mu\text{g/L}$)	PBC ($\mu\text{mol/L}$)	B3CAs ($\mu\text{g/L}$)	B4CAs ($\mu\text{g/L}$)	B5CAs ($\mu\text{g/L}$)	B6CAs ($\mu\text{g/L}$)	PBC ($\mu\text{mol/L}$)
1	0.57	6.19	7.41	8.47	10.75	0.07	0.73	0.78	0.92	1.18
2	0.19	1.65	2.11	2.26	2.94	0.05	0.48	0.56	0.81	0.90
3	2.70	24.00	26.85	25.87	37.72	0.15	1.94	2.83	2.08	3.32
4	0.80	3.55	3.39	3.09	5.15	0.19	2.80	3.60	3.37	4.73
5	0.76	1.89	1.67	1.54	2.78	0.78	10.98	11.79	13.27	17.49
6	0.74	1.29	0.94	0.97	1.87	0.10	1.20	1.50	1.53	2.05
7	1.11	1.71	1.21	1.27	2.51	0.13	1.60	1.80	2.03	2.64
8	1.63	10.66	8.58	9.84	14.58	0.79	11.94	10.32	16.05	18.58
Average	1.06 \pm 0.78	6.37 \pm 7.81	6.52 \pm 8.71	6.66 \pm 8.47	9.79 \pm 12.17	0.28 \pm 0.31	3.96 \pm 4.69	4.15 \pm 4.40	5.01 \pm 6.06	6.36 \pm 7.31

Table S4. Dual-carbon isotopic compositions ($\Delta^{14}\text{C}$ - $\delta^{13}\text{C}$) and ^{14}C ages of DBC and PBC at the forest and urban sites.

Compounds	DBC						PBC						
	Wet Season		Dry Season		Mix Season		Wet Season		Dry Season		Mix Season		
	Forest site	Urban site	Forest site	Urban site	Forest site	Urban site	Forest site	Urban site	Forest site	Urban site	Forest site	Urban site	
$\delta^{13}\text{C}$ (‰)	B6CA	-29.26 ± 0.39	-27.56 ± 0.40	-29.41 ± 0.39	-27.31 ± 0.40	-29.47 ± 0.42	-27.96 ± 0.39	-25.73 ± 0.39	-21.02 ± 0.39	-29.12 ± 0.45	-24.70 ± 0.39	-24.95 ± 0.39	-22.67 ± 0.41
	B5CA	-29.33 ± 0.22	-27.72 ± 0.24	-27.11 ± 0.23	-27.43 ± 0.27	-28.52 ± 0.23	-27.72 ± 0.22	-25.80 ± 0.22	-21.93 ± 0.23	-26.14 ± 0.23	-22.36 ± 0.23	-24.84 ± 0.22	-23.20 ± 0.22
	B4CAs	-28.51 ± 0.18	-27.50 ± 0.21	-28.91 ± 0.18	-27.47 ± 0.23	-29.07 ± 0.18	-27.73 ± 0.18	-27.70 ± 0.19	-23.46 ± 0.18	-30.45 ± 0.18	-25.12 ± 0.19	-26.05 ± 0.18	-25.70 ± 0.18
	$\delta^{13}\text{C}_{\text{BC}}^{\text{a}}$	-28.92 ± 0.49	-27.60 ± 0.52	-28.26 ± 0.49	-27.44 ± 0.53	-28.90 ± 0.51	-27.75 ± 0.49	-26.36 ± 0.49	-22.16 ± 0.49	-28.59 ± 0.54	-24.23 ± 0.49	-25.24 ± 0.49	-24.04 ± 0.50
	B6CA	-2.0 ± 14.8	-182.9 ± 6.9	-12.3 ± 21.2	-220.7 ± 8.2	-5.1 ± 15.2	-152.7 ± 8.4	-172.8 ± 17.6	-362.5 ± 13.2	-345.6 ± 52.8	-599.3 ± 11.8	-98.6 ± 17.3	-354.9 ± 35.9
$\Delta^{14}\text{C}$ (‰)	B5CA	-36.0 ± 12.1	-134.5 ± 3.6	-4.9 ± 16.7	-163.0 ± 4.1	-2.6 ± 11.2	-121.8 ± 3.4	-44.8 ± 29.1	-187.1 ± 34.7	n.d.	-294.3 ± 96.3	3.5 ± 51.5	-190.7 ± 143.4
	B4CAs	-65.7 ± 12.0	-282.8 ± 2.7	-71.7 ± 14.5	-312.2 ± 2.8	-38.9 ± 11.0	-239.9 ± 3.1	-177.8 ± 55.1	-320.5 ± 36.1	-145.5 ± 126.8	-392.3 ± 63.2	-66.1 ± 48.4	-329.8 ± 119.6
	$\Delta^{14}\text{C}_{\text{BC}}^{\text{a}}$	-46.7 ± 7.8	-210.9 ± 2.1	-39.3 ± 10.1	-245.8 ± 2.3	-20.2 ± 7.2	-182.7 ± 2.2	-134.5 ± 20.4	-290.4 ± 17.5	-245.5 ± 68.7	-418.3 ± 39.9	-54.5 ± 23.5	-292.1 ± 67.0
	^{14}C ages	386 ± 71	1934 ± 22	328 ± 87	2300 ± 25	166 ± 65	1641 ± 24	1177 ± 197	2796 ± 196	2334 ± 683	5211 ± 543	467 ± 198	2811 ± 745

193 ^a $\delta^{13}\text{C}_{\text{BC}}$ and $\Delta^{14}\text{C}_{\text{BC}}$ were calculated based on mass balance using the abundances and $\delta^{13}\text{C}$ and $\Delta^{14}\text{C}$ values of individual BPCAs.

194 n.d.: No $\Delta^{14}\text{C}$ data was reported for dry-season PBC because the B5CA yield was insufficient for reliable $\Delta^{14}\text{C}$ measurement.

Table S5. Information on eight sampling sites during the first sampling campaign.

Sample ID From upstream to downstream	Longitude (°E)	Latitude (°N)
1	113.72	23.72
2	113.66	23.66
3	113.60	23.55
4	113.52	23.49
5	113.44	23.42
6	113.35	23.41
7	113.30	23.34
8	113.20	23.25

197 **Table S6. Binary gradient of HPLC method for BPCA quantification.** (Mobile
198 phase A: 2% H₃PO₄ in ultrapure water; Mobile phase B: 100% acetonitrile. Flow rate
199 = 0.4 mL/min)

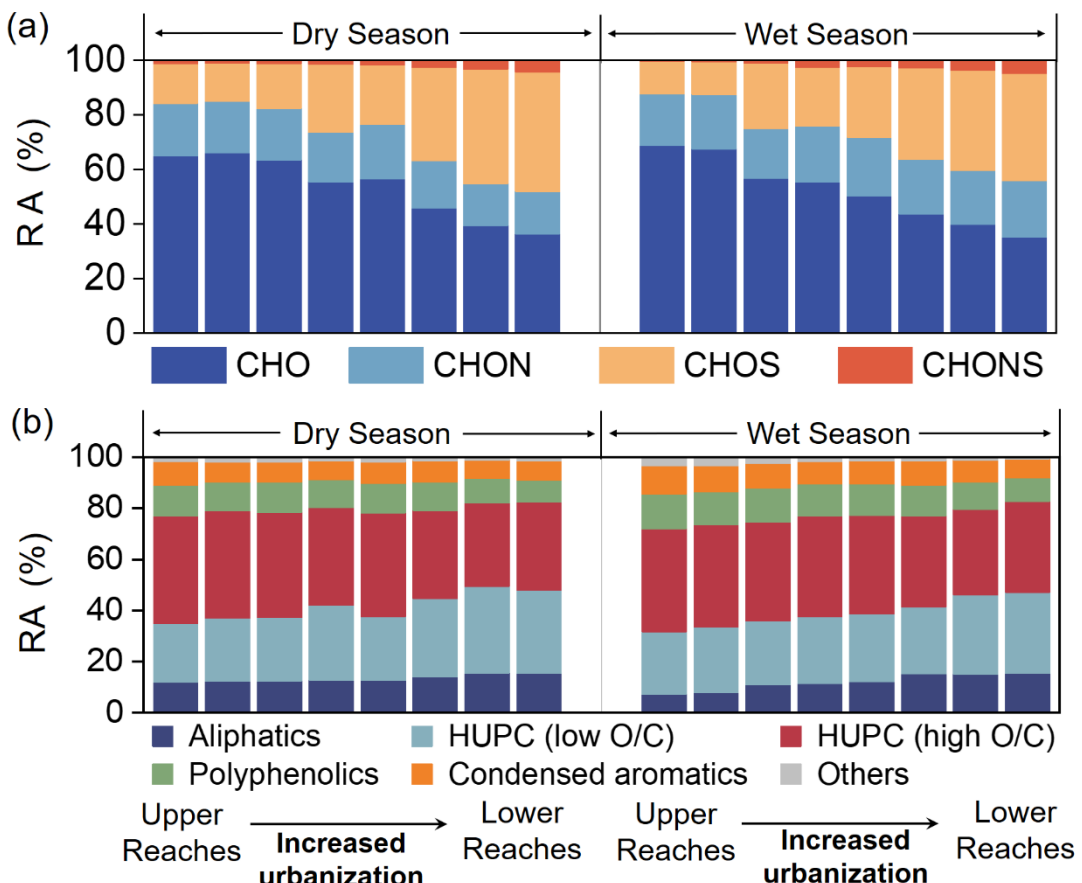
Time (min)	Mobile phase B (vol %)
0	0.5
5	0.5
25.9	30
26	95
28	95
28.1	0.5
30	0.5
50.5	0.5

200

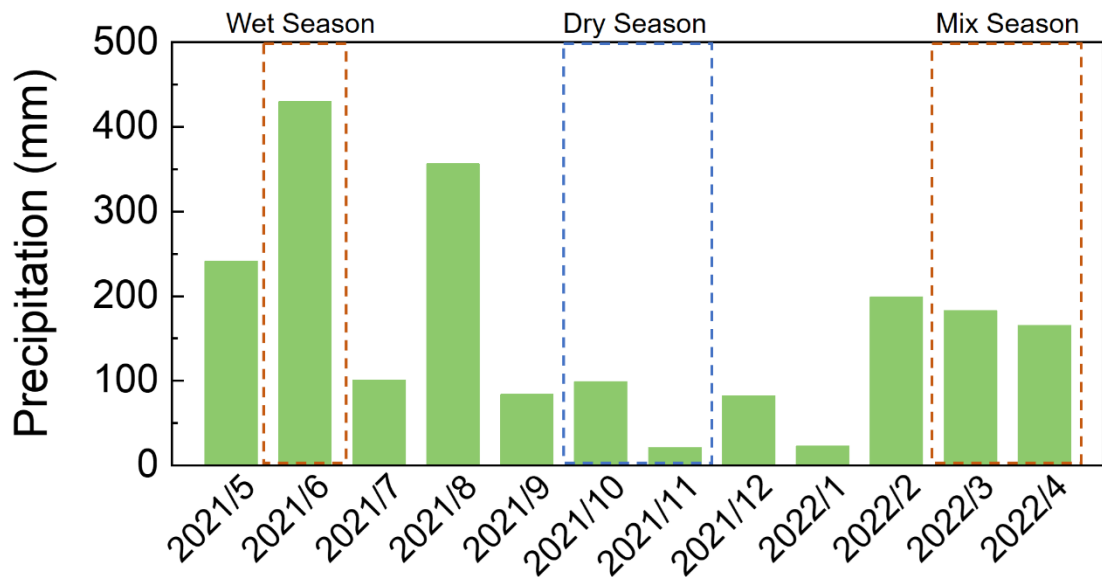
201 **Table S7. Binary gradient of preparative high-performance liquid**
202 **chromatography (prep-HPLC).** (Mobile phase A: 0.38% TFA in ultrapure water;
203 Mobile phase B: 100% acetonitrile. Flow rate = 0.4 mL/min)

Time (min)	Mobile phase B (vol %)
0	0.5
5	0.5
18	20
37.9	30
38	95
40	95
40.1	0.5
62.01	0.5

204



207 **Figure S1.** DOM molecular compositions along the urbanization gradient of the Liuxi
 208 River. (a) The relative abundance (RA) of CHO-, CHON-, CHOS- and CHONS-
 209 containing formulae. (b) The relative abundance (RA) of four groups of compounds,
 210 including aliphatic compounds, highly unsaturated and phenolic compounds (HUPs)
 211 (low oxygen), HUPs (high oxygen), polyphenolic compounds, and condensed aromatic
 212 compounds.



214

215 **Figure S2.** Monthly precipitation during the second sampling campaign (May 2021 to
216 April 2022) of Guangzhou (Baiyun International Station, 23.39°N, 113.30°E). The data
217 were obtained from <https://www.ncei.noaa.gov/maps/daily/>.

218

219 **References**

220 (1) Dittmar, T.; Koch, B.; Hertkorn, N.; Kattner, G. A simple and efficient method for
221 the solid-phase extraction of dissolved organic matter (SPE-DOM) from seawater.
222 *Limnol. Oceanogr.: Methods* **2008**, 6, 230-235. DOI: 10.4319/lom.2008.6.230.

223 (2) Meier-Augenstein, W.; Schimmelmann, A. A guide for proper utilisation of stable
224 isotope reference materials*. *Isot. Environ. Health Stud.* **2019**, 55 (2), 113 - 128.

225 (3) Santos, G. M.; Southon, J. R.; Druffel-Rodriguez, K. C.; Griffin, S.; Mazon, M.
226 Magnesium perchlorate as an alternative water trap in AMS graphite sample preparation:
227 A report on sample preparation at KCCAMS at the University of California, Irvine.
228 *Radiocarbon* **2004**, 46 (1), 165-173. DOI: 10.1017/s0033822200039485.

229 (4) Zhu, S.; Ding, P.; Wang, N.; Shen, C.; Jia, G.; Zhang, G. The compact AMS facility
230 at Guangzhou Institute of Geochemistry, Chinese Academy of Sciences. *Nucl Instrum
231 Meth B* **2015**, 361, 72-75. DOI: 10.1016/j.nimb.2015.06.040.

232 (5) Koch, B. P.; Dittmar, T. From mass to structure: an aromaticity index for high-
233 resolution mass data of natural organic matter. *Rapid Commun. Mass Spectrom.* **2006**,
234 20 (5), 926-932, Article. DOI: 10.1002/rcm.2386.

235 (6) Koch, B. P.; Dittmar, T. From mass to structure: an aromaticity index for high-
236 resolution mass data of natural organic matter. *Rapid Commun. Mass Spectrom.* **2016**,
237 30 (1), 250-250. DOI: <https://doi.org/10.1002/rcm.7433>.

238 (7) Jiang, H.; Tang, J.; Li, J.; Zhao, S.; Mo, Y.; Tian, C.; Zhang, X.; Jiang, B.; Liao, Y.;
239 Chen, Y.; et al. Molecular Signatures and Sources of Fluorescent Components in
240 Atmospheric Organic Matter in South China. *Environ. Sci. Technol. Lett.* **2022**, 9 (11),
241 913-920. DOI: 10.1021/acs.estlett.2c00629.

242 (8) Mo, Y.; Li, J.; Zhong, G.; Zhu, S.; Cheng, Z.; Tang, J.; Jiang, H.; Jiang, B.; Liao, Y.;
243 Song, J.; et al. The Sources and Atmospheric Processes of Strong Light-Absorbing
244 Components in Water Soluble Brown Carbon: Insights From a Multi-Proxy Study of
245 PM2.5 in 10 Chinese Cities. *J. Geophys. Res.: Atmos.* **2024**, 129 (2), e2023JD039512.
246 DOI: <https://doi.org/10.1029/2023JD039512>.

247 (9) Sun, Y.; Tang, J.; Mo, Y.; Geng, X.; Zhong, G.; Yi, X.; Yan, C.; Li, J.; Zhang, G.
248 Polycyclic Aromatic Carbon: A Key Fraction Determining the Light Absorption

249 Properties of Methanol-Soluble Brown Carbon of Open Biomass Burning Aerosols.
250 *Environ. Sci. Technol.* **2021**, *55* (23), 15724-15733. DOI: 10.1021/acs.est.1c06460.

251 (10) Geng, X.; Zhong, G.; Liu, J.; Sun, Y.; Yi, X.; Bong, C. W.; Zakaria, M. P.;
252 Gustafsson, Ö.; Ouyang, Y.; Zhang, G. Year-Round Measurements of Dissolved Black
253 Carbon in Coastal Southeast Asia Aerosols: Rethinking Its Atmospheric Deposition in
254 the Ocean. *J. Geophys. Res.: Atmos.* **2021**, *126* (18), e2021JD034590. DOI:
255 10.1029/2021JD034590.

256 (11) Vaezzadeh, V.; Yi, X.; Thomes, M. W.; Bong, C. W.; Lee, C. W.; Zakaria, M. P.;
257 Wang, A.-J.; Roslin, P. N. B.; Zhong, G.; Zhang, G. Use of molecular markers and
258 compound-specific isotopic signatures to trace sources of black carbon in surface
259 sediments of Peninsular Malaysia: Impacts of anthropogenic activities. *Mar. Chem.*
260 **2021**, *237*, 104032. DOI: 10.1016/j.marchem.2021.104032.

261 (12) Hanke, U. M.; Wacker, L.; Haghipour, N.; Schmidt, M. W. I.; Eglinton, T. I.;
262 McIntyre, C. P. Comprehensive radiocarbon analysis of benzene polycarboxylic acids
263 (BPCAs) derived from pyrogenic carbon in environmental samples. *Radiocarbon* **2017**,
264 *59* (4), 1103-1116. DOI: 10.1017/rdc.2017.44.

265 (13) Yi, X.; Zhong, G.; Geng, X.; Tang, J.; Lin, B.; Zhu, S.; Gao, S.; Yao, C.; Cheng,
266 Z.; Zhao, S.; et al. Dual-carbon isotope analysis of benzene polycarboxylic acids for
267 tracking black carbon across different environments. *Appl. Geochem.* **2024**, *170*,
268 106062. DOI: <https://doi.org/10.1016/j.apgeochem.2024.106062>.

269 (14) Wiedemeier, D. B.; Lang, S. Q.; Gierga, M.; Abiven, S.; Bernasconi, S. M.; Fruh-
270 Green, G. L.; Hajdas, I.; Hanke, U. M.; Hilf, M. D.; McIntyre, C. P.; et al.
271 Characterization, Quantification and Compound-specific Isotopic Analysis of
272 Pyrogenic Carbon Using Benzene Polycarboxylic Acids (BPCA). *Jove-Journal of*
273 *Visualized Experiments* **2016**, (111), e53922. DOI: 10.3791/53922.

274 (15) Zhong, G.; Sun, Y.; Geng, X.; Yi, X.; Zhang, G. Benzene polycarboxylic acid
275 characterisation of polyaromatics in ambient aerosol: Method development. *Atmos.*
276 *Environ.* **2019**, *211*, 55-62. DOI: 10.1016/j.atmosenv.2019.04.057.

277 (16) Vaezzadeh, V.; Yi, X.; Rais, F. R.; Bong, C. W.; Thomes, M. W.; Lee, C. W.; Zakaria,
278 M. P.; Wang, A. J.; Zhong, G.; Zhang, G. Distribution of black carbon and PAHs in
279 sediments of Peninsular Malaysia. *Mar. Pollut. Bull.* **2021**, *172*. DOI:
280 10.1016/j.marpolbul.2021.112871.

281 (17) Dittmar, T. The molecular level determination of black carbon in marine dissolved
282 organic matter. *Org. Geochem.* 2008, 39 (4), 396-407. DOI:
283 10.1016/j.orggeochem.2008.01.015.

284